Damage Simulation in Non-Crimp Fabric Composite Plates Subjected to Impact loads

Authors: Arunkumar Satyanarayana
Philip B. Bogert
Venkat Aitharaju
Satvir Aashat
Hamid Kia

ABSTRACT

Progressive failure analysis (PFA) of non-crimp fabric (NCF) composite laminates subjected to low velocity impact loads was performed using the COmplete STress Reduction (COSTR) damage model implemented through VUMAT and UMAT41 user subroutines in the frame works of the commercial finite element programs ABAQUS/Explicit and LS-DYNA, respectively. To validate the model, low velocity experiments were conducted and detailed correlations between the predictions and measurements for both intra-laminar and inter-laminar failures were made. The developed material and damage model predicts the peak impact load and duration very close with the experimental results. Also, the simulation results of delamination damage between the ply interfaces, in-plane matrix damages and fiber damages were all in good agreement with the measurements from the non-destructive evaluation data.

Arunkumar Satyanarayana, Analytical Mechanics Associates Inc., 21 Enterprise Parkway Suite 300, Hampton, VA 23666-6413, U.S.A.
Philip B. Bogert, NASA Langley Research Center, Mail Stop 190, Hampton, VA 23681, U.S.A.
Venkat Aitharaju, Satvir Aashat, Hamid Kia, General Motors Company, Global R & D Center, Warren, MI 48090, U.S.A.

INTRODUCTION

Carbon fiber composite materials are being widely used in aerospace applications and are being slowly introduced into the automobile industry to achieve better fuel economy, increased durability and improved driving experience. Optimizing the weight of an automobile is a significant factor in achieving higher fuel economy, and to that end, composite materials are very promising due to their low densities. Among the carbon fiber composite materials under consideration, the non-crimp fabric (NCF) preform is an attractive alternative to the traditional pre-pregnated tapes due to its low manufacturing cost and high efficiency. The NCF material consists of multiple layers of unidirectional plies oriented at varying angles which are held together by transverse stitches. A typical carbon fiber NCF composite laminate is shown in Figure 1.

Figure 1: Photograph of a typical Non-Crimp Fabric (NCF) laminate.

Since the use of NCF composites is gaining momentum, researchers are developing novel computational methods to evaluate the performance of these materials under varying load conditions. Researchers in Refs. [1-3] have developed micro, macro and meso-scale material models to evaluate some of the material properties and strengths, which are extremely difficult to obtain by standard material characterization tests. In Refs. [4-5], researchers have developed a meso-scale plane stress damage model to simulate damage in NCF cross-ply laminates subjected to tension and compressive loads. The influence of out-of-plane imperfections in the NCF laminate due to the misalignment of the fibers was investigated in Ref. [5]. The extent of damage in a NCF composite sandwich panel under impact load was established using an ultrasonic C-scan in Ref. [6].

Even though a good amount of research has been performed in simulating the damage progression in tape laminates subjected to impact loads [7-11], less effort has been dedicated to NCF composite laminates. Hence, in the present investigation, a 2D stress damage model called COmplete STress Reduction (COSTR), previously developed for fiber and matrix damage predictions in tape laminates by the authors from NASA [12] for in-plane loads, was extended to out-of-plane loads for thin NCF laminates. This damage model will be implemented in the framework of the

commercial software packages ABAQUS and LS-DYNA. Though this approach was first developed for use in Abaqus for the aerospace industry, because the automotive industry relies heavily on LS-DYNA, the damage models developed for NCF composites will be incorporated into both codes. In this manner it is anticipated that large real world problems such as the progressive failure of aircraft wings and fuselages, and crash of automobiles, can be simulated. NCF material preparation and low velocity dynatup impact tests were conducted at the General Motors R & D Facility. Progressive failure analysis (PFA) of the NCF laminate, impacted by a hemispherical impactor at 5J, 10J & 12J energy levels was performed and analysis predictions for the overall panel response, such as impact load versus time duration, were compared with the experimental results. Fiber damages within the plies and delamination damages between the layers were compared with X-ray and CT-scan data.

PROGRESSIVE FAILURE ANALYSIS – DAMAGE MODELS

During the low velocity impacts, composites are subjected to both intra-laminar and inter-laminar failures. Intra-laminar failures were studied previously for in-plane loads utilizing the COSTR damage model developed and implemented through a VUMAT user subroutine in ABAQUS/Explicit [12] for tape laminates. The inter-laminar failure, referred to here as delamination failure occurring between the layers of a composite, poses a major challenge for damage prediction and thus requires an advanced modeling strategy. A brief description of the damage model will be outlined here. For a detailed description of the model, readers are referred to refs. [12-13].

Intra-Laminar Damage Model

The COSTR damage model for intra-laminar damage utilizes the Hashin-Rotem unidirectional failure criteria [14] to detect fiber and matrix damages in a lamina. The failure criteria are expressed in terms of the in-plane stresses σ_{ij}, the strengths in tension, X, compression, Y, and shear, S_{XY}, respectively. Two damage indices d_F and d_M are used to represent the fiber and matrix damage modes, respectively. Each damage index has the value of zero (no damage) or 1.0 (complete damage). The previous stress degradation model, adopted to degrade the axial (σ_{11}), transverse (σ_{22}), and shear (σ_{12}) stresses as a function of axial (ε_{11}), transverse (ε_{22}), and shear (ε_{12}) strains respectively, after they reach their failure limits at a material point is shown in Figure 2(a). When the damage parameter d_M attains a value of 1.0, both the transverse and the shear stresses were reduced to zero instantaneously. Similarly, when the damage parameter d_F attains a value of 1.0, all of the in-plane and shear stresses at that material point were made zero. This type of instantaneous stress degradation to zero is characterized as a single-step or instantaneous degradation approach and hence the model was assigned the name COmplete STress Reduction (COSTR) damage model. This type of stress degradation approach is suitable for performing PFA of un-configured laminated composite panels under quasi static loading conditions. But, while analyzing configured panels (skin-stringer) or structures under dynamic loading conditions, this stress degradation approach generates an extremely large energy release in the model thereby causing all the elements along the crack paths to fail

instantaneously. This phenomenon has been studied and reported in Ref. [14]. To circumvent the above difficulties, the fiber stresses in the failed material point are reduced to a nominal percentage of the original strength (20% or so), and these stresses are maintained until the strain in the fiber direction reaches a value of 2.5 times the elastic strain (ε^{el}_{11}) of the fiber. However, the transverse and shear stresses are still degraded to zero instantaneously after the failure as they do not pose difficulties in the simulation. The stress degradation model used in the present study is shown in Figure 2(b).

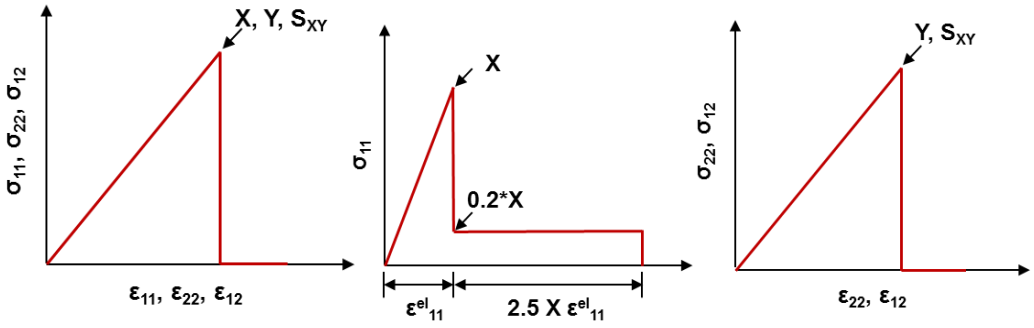

a) Previous Approach b) Current Approach

Figure 2. Stresses degradation approaches in COSTR damage model.

Another characteristic of the COSTR damage model that differs from the standard ABAQUS/LS-DYNA damage model is the elimination of the influence of Poisson's ratio in evaluating the axial stress in the fibers when the matrix has failed due to the transverse tension/compression or shear stress. It has been observed during the study that in some plies of a laminate, the transverse strain, shear strain or the combination of transverse and shear strains could result in significant distortion of the element without significant stress in the fiber direction. An example of this phenomenon is a laminate consisting of 90° plies and loaded in the direction perpendicular to the fibers. To avoid excessive distortion of an element, a quadratic strain criterion, was formulated and implemented in the damage evolution procedure of the PFA methodology to eliminate badly distorted elements from the simulation. The matrix strain failure criterion (MSFC) is defined as

$$MSFC = \sqrt{(\varepsilon_{22})^2 + (\gamma_{12})^2}$$

When the MSFC at a material point reaches a significant value, approximately 0.25, the material point is deleted. Once a material point is deleted it cannot be reactivated. The ABAQUS and LS-DYNA explicit solvers check for elements where all of the material points have been flagged as deleted and then, these elements are removed from further computations, thereby simulating virtual cracks in the finite element model. The COSTR damage model has been implemented through the VUMAT and UMAT41 [15] user written subroutines in the ABAQUS and LS-DYNA codes, respectively.

Inter-Laminar Damage Model

The simulation of inter-laminar damage, i.e., delamination, between the sublaminate layers was accomplished using the cohesive zone model available in the ABAQUS and LS-DYNA computer programs. The onset of delamination was determined based on the inter-laminar quadratic normal and shear stress criterion and the delamination growth was based on a critical fracture energy criterion. Damage was modeled as an irreversible process by including a damage parameter and this parameter is directly related to the dissipated fracture energy. A detailed explanation of the cohesive zone model can be found in Ref. [13]. Among the analysis parameters for the cohesive layers, stiffness of the cohesive layer is an important parameter for the simulation, as lower stiffness values can make the laminate too compliant and higher stiffness values can cause spurious oscillations of the tractions in the element introducing numerical difficulties. Ref [16] provides the guidelines for stiffness determination and one such guideline for the mode-1 direction is given below:

$$K_I \approx \left(\frac{\alpha E_3}{t} \right)$$

where E_3 is the Young's modulus of the laminate in the thickness direction, t is the larger of the sub-laminate thicknesses above or below the cohesive layer, and α is a parameter that is much larger than 1. A value of α equal to 50 is recommended in Ref. [15] and was used in the current study to obtain a stiffness of the cohesive layer. In calculating the stiffnesses K_{II} and K_{III} for the mode-1 and mode-2 directions, E_3 is replaced in the above equations with the shear moduli G_{12} and G_{13} of the laminate, respectively.

DESCRIPTION OF NCF COUPON AND TEST SETUP

An eight layer carbon fiber non-crimp fabric with a quasi-isotropic layup (0/ -45/45/90/90/45/-45/0) from Sigmatex was used to manufacture plates with dimensions 431.8 x 431.8 x 1.8 mm at the General Motors Research Labs using resin transfer molding. The NCF fabric was made from T700 grade fiber. An epoxy resin with a fast curing agent was used for the resin transfer molding of the composite. The volume fraction of carbon fiber was determined to be close to 48%. Basic material characterization tests for stiffness and strength were conducted following ASTM standards to obtain the material properties in tension, compression, and shear. The material properties are listed in Table I. These material properties were validated by correlating the results with a three point bend test. For the low velocity impact tesing, square specimens of 101.6 mm wide were cut from the manufactured plates of NCF and were subjected to an impact using an INSTRON dynatup testing machine, equipped with a digital acquisition system. The test-specimen was restrained using a clamping fixture (upper and lower plates) which exposed a circular area of 76.2 mm diameter, and then impacted by a rigid tup at the center of the exposed area. A hemispherical steel impactor with a diameter of 25.4 mm and a weight of 7.0 kg was used. Three levels of energy input (5J, 10 J and 12J) were studied. The test setup is shown in Figure 3.

TABLE I. MATERIAL PROPERTIES OF NCF COUPONS

Properties	T700/Epoxy	Description
E_{11} (GPa)	102.0	Young's modulus in fiber direction
E_{22} (GPa)	7.08	Young's modulus in the transverse direction
G_{12} (GPa)	3.16	In-plane shear modulus
S_{11} (GPa)	1.63	Tensile strength in the fiber direction
C_{11} (GPa)	1.43	Compressive strength in the fiber direction
S_{22} (GPa)	0.068	Tensile strength in the transverse direction
C_{22} (GPa)	0.30	Compressive strength in the transverse direction
S_{12} (GPa)	0.05	In-plane shear strength
ν_{12}	0.4	Poisson's Ratio
G_{Ic} (J/m2)	1062.0	Critical Fracture toughness in Mode 1 Direction
G_{IIc}, G_{IIIc} (J/m2)	1276.0	Critical Fracture toughness in Mode 2 & 3 directions

The cohesive damage model available in ABAQUS and LS-DYNA was used in simulating delaminations between the sublaminate layers. The interfacial stiffness and strength parameters used in the analysis are given in Table II.

TABLE II. INTERLAMINAR PROPERTIES AND STRENGTH DATA

Properties	T700/Epoxy	Description
K_{11} (GPa)	781.4	Interfacial Stiffness in Mode 1 direction
K_{12} (GPa)	360.1	Interfacial Stiffness in Mode 2 direction
K_{22} (GPa)	360.1	Interfacial Stiffness in Mode 3 direction
S_{33} (GPa)	0.06895	Interfacial strength in Mode 1 direction
S_{13} (GPa)	0.08274	Interfacial strength in Mode 2 direction
S_{32} (GPa)	0.08274	Interfacial strength in Mode 2 direction

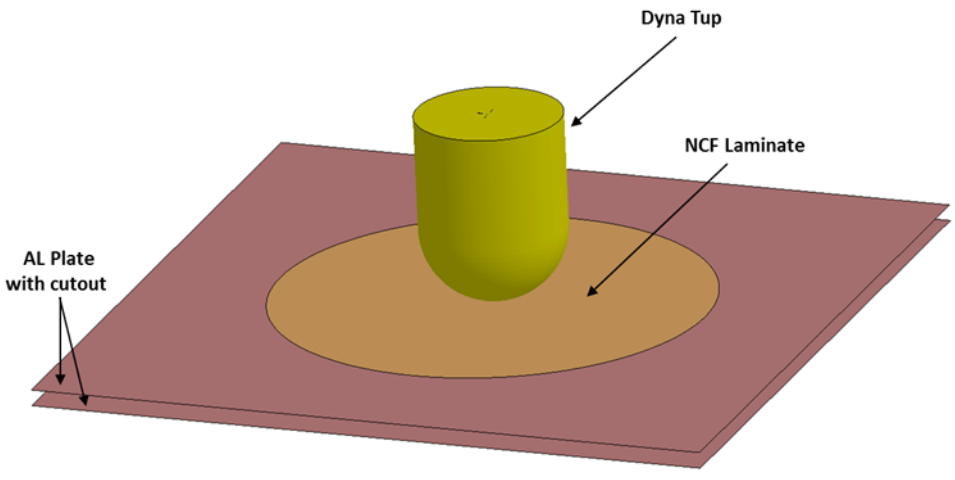

Figure 3: Assembly of Non-Crimp Fabric (NCF) laminate & AL plate with cutouts.

FINITE ELEMENT MODEL DESCRIPTION

A three-dimensional (3D) finite element model of the square plate was developed to simulate the coupled inter- and intra-laminar damage. The thickness of the model was divided into five sub-laminate sections with a cohesive layer of zero thickness between each of them. The pictorial representation of the plate model, which consists of sub-laminate sections and the cohesive layers, is shown in Figure 4(a). The finite element mesh for each of the sub-laminates and the cohesive layers is shown in Figure 4(b). Each sublaminate layer was modeled using one solid element in the thickness direction. The sub-laminate sections were discretized using the 8-node continuum shell reduced integration element (SC8R) available in the ABAQUS™ element library [13] and continuum solid elements in LS-DYNA. The SC8R element is a 3D element with translational degrees-of-freedom (DOF) using only linear interpolation functions. It differs from a 3D solid element in that it employs composite lamination theory and therefore provides an ability to discretize 3D bodies with multiple sublaminates through the thickness. The element size used in discretizing the planar regions of the sub-laminates ranges from 0.5 mm by 0.5 mm in the center under the impactor to a size of 1.5 mm by 1.5mm close to the edges of the plate. The cohesive layers were modeled using a zero thickness ABAQUS™ 8-node cohesive element known as COH3D8 [16], and in LS-DYNA, cohesive elements were defined with material model MAT_COHESIVE_MIXED_MODE. An in-plane discretization of 0.5 by 0.5 mm was used in the cohesive layers. The sub-laminate sections and the cohesive layers were connected using ABAQUS™ and LS-DYNA "tie" boundary conditions, in each approach respectively, to maintain the continuity between the sub-laminate sections before the damage occurs. The assemblage of the five sub-laminate sections and four cohesive layers through the thickness defines the complete plate model.

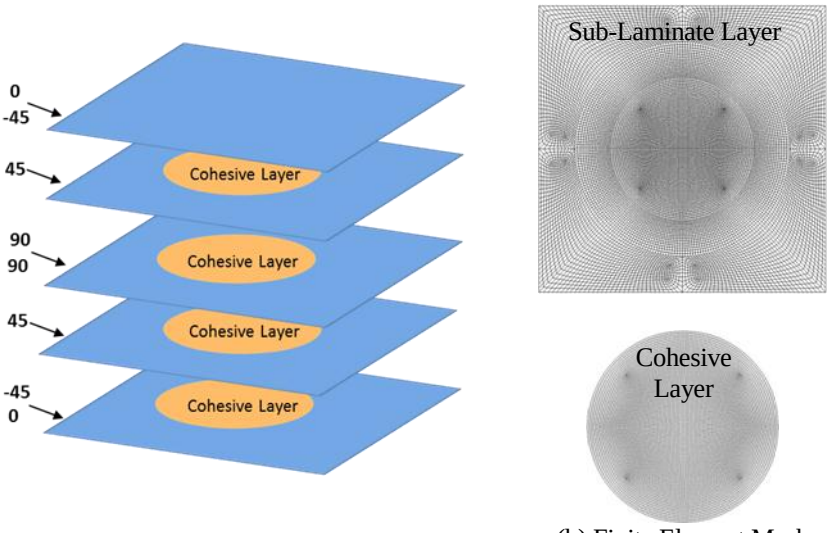

(a) Schematic Diagram of Sub-laminate & Cohesive layers

(b) Finite Element Mesh

Figure 4: Modeling procedure of NCF plate & finite element mesh.

The nodes on the sublaminate surfaces which are in contact with the top and bottom support plates were constrained in the out of plane direction only. Additional boundary conditions were applied to the nodes along the vertical and horizontal center

lines of all the sublaminate layers as shown in Figure 5 in order to suppress spurious element distortions due to shock waves. The plate was impacted with an impactor at an initial velocities of 1.12 m/sec, 1.68 m/sec and 1.85 m/sec to produce the desired 5J, 10J and 12J energy levels.

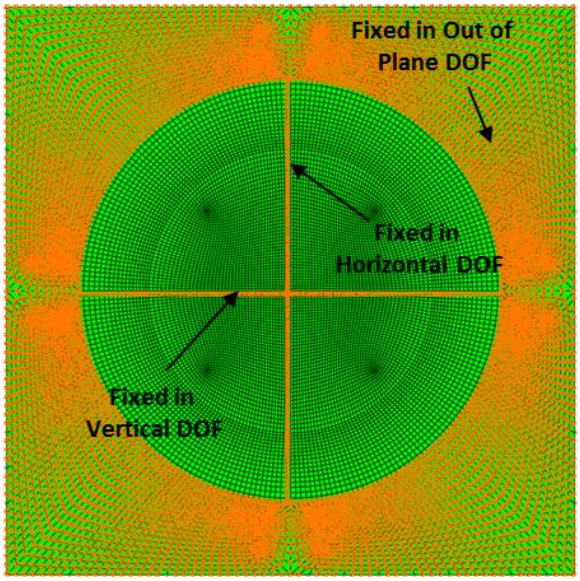

Figure 5: Finite element mesh with prescribed boundary conditions.

The impact simulation was performed using the ABAQUS™ and LS-DYNA explicit double precision solvers for each of the energy levels. Since the plate is severely constrained and the effective width of plate was rather small, the elements under the impactor can show spurious hour-glass modes due to the under integrated elements. Hence, an additional viscous stiffness was added in all the sublaminate elements to eliminate zero energy modes in the plate in the respective codes.

RESULTS AND DISCUSSION

PFA results such as impact load history and delamination damage at certain critical interfaces of the NCF plate for the impact energy levels of 5J, 10J & 12J are compared with experimental test results in the following sections. For the sake of brevity, the comparative simulation results for LS-DYNA and the ABAQUS/COSTR damage model were presented only for the 5J test case.

5J Impact Energy

The load history curves obtained from the PFA and two tests for the 5J energy level impact cases are presented in Figure 6. From Figure 6, it can be noticed that the contact duration and the peak impact load obtained from the analysis (green) are in good agreement with the test data (purple). The raw load history curve from the analysis was oscillatory, due to the contact disturbances occurring in the simulation. These oscillations in the load were smoothened by passing it through filters provided in the ABAQUS post processing tool.

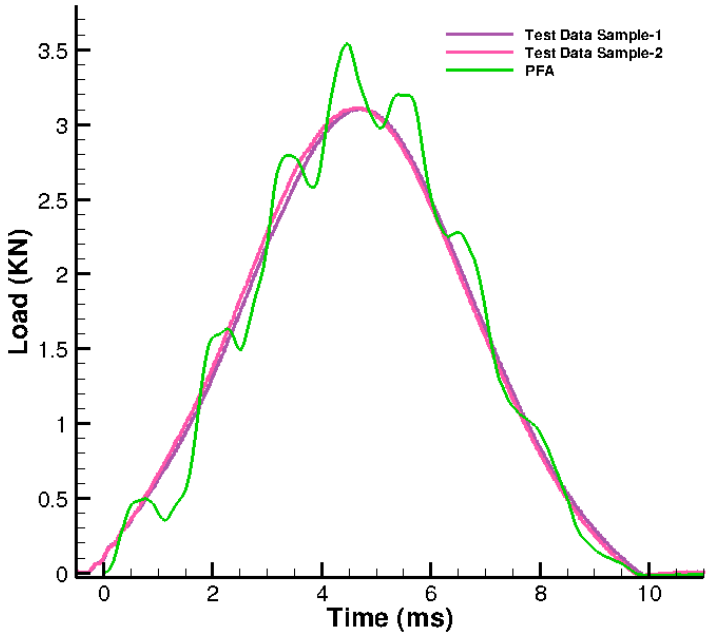

Figure 6: Comparison of load versus time curve from ABAQUS/VUMAT simulation and dynatup experiment

Figure 7 presents the comparison of load history curves for the LS-DYNA user defined COSTR damage model and test results. It can be observed that the damage model implemented in LS-DYNA provides excellent correlation with the experimental results and also agrees well with the ABAQUS/COSTR simulation. A 7 point averaging available in the LSPOST program was used to smooth the contact force curves.

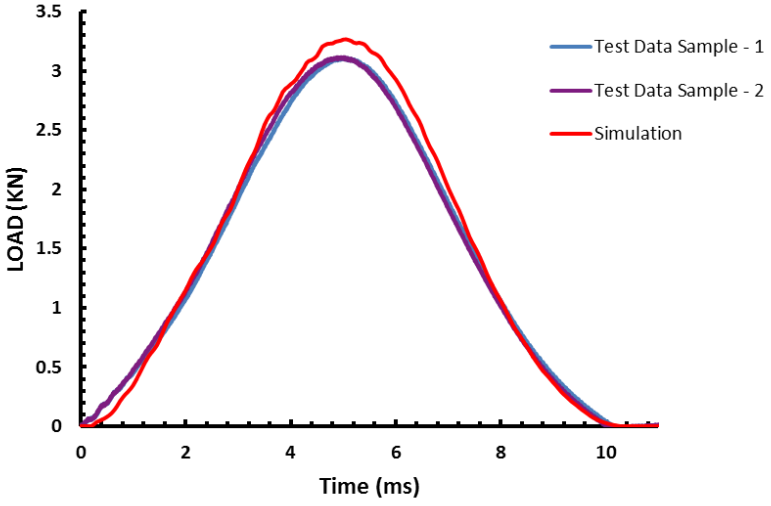

Figure 7: Comparison of load versus time curve from LS-DYNA UMAT 41 simulation and dynatup experiment

The simulated delamination at certain critical ply interfaces for the 5J impact load is presented in Figure 8, along with the NDE ultrasound measurements. The general orientation of the delamination damage showed fair agreement at the various interfaces in comparison with the NDE data. The layers in the NCF plate are numbered such that the layer that comes in contact with the impactor was numbered as layer 1 and the bottom most layer was numbered as layer 8. The cummulative delamination through the entire thickness from the ABAQUS/VUMAT simulation was compared with the damage measured using ultrasound NDE techniques and is shown in Figure 9(a). From the figure, good agreement is observed between the predictions and the experimental measurements. Similarly, the simulation results for the cumulative delamination in the laminate from the LS-DYNA/UMAT41 simulation was compared with ultrasound NDE results and presented in Figure 9(b). A good correlation with the experiment and both the simulation results was observed, confirming a successful implementation of the COSTR damage model in the LS-DYNA code. In all of the delamination pictures below, the region in white indicates a complete delamination of interfaces, the region in red indicates areas which are 95% of complete delamination and the region in blue implies an intact bonding of the interfaces.

No fiber failure was predicted in any of the plies in the simulations, matching the experimental observations. The matrix damage predicted from the simulation in the elements was not significant, and hence, is not presented.

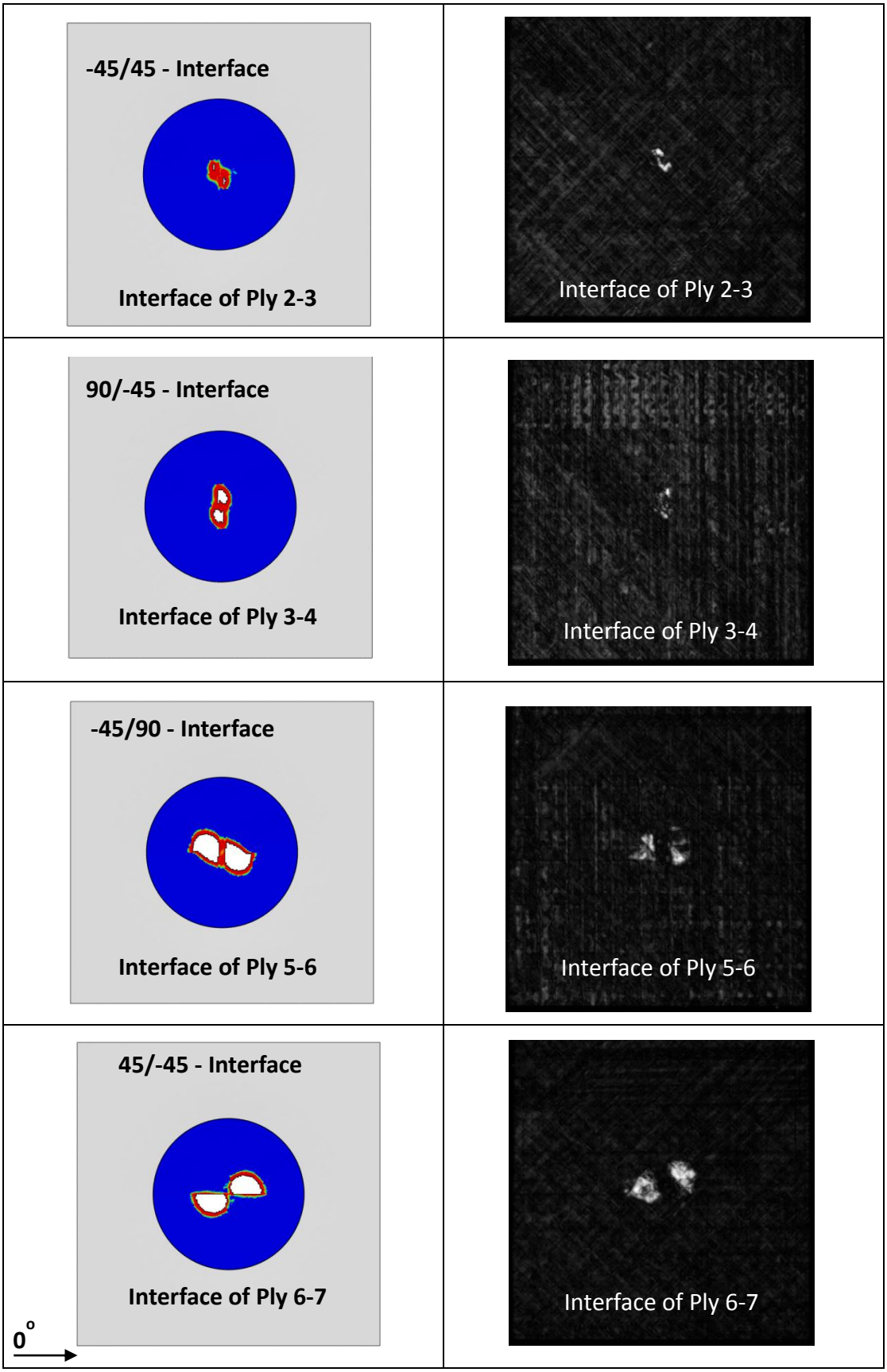

Figure 8: Delamination at certain interfaces. Left hand side - PFA, Right hand side - NDE technique.

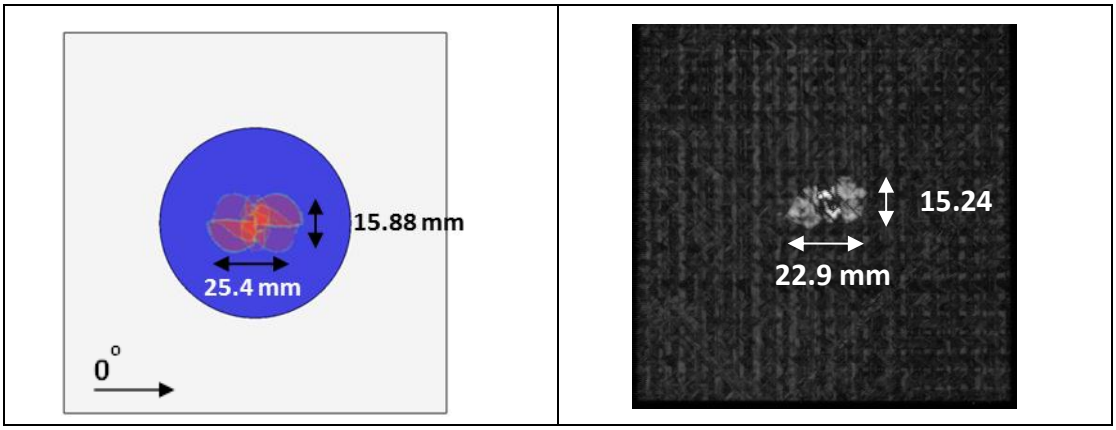

(a): Left hand side – ABAQUS/VUMAT simulation, Right hand side - NDE technique.

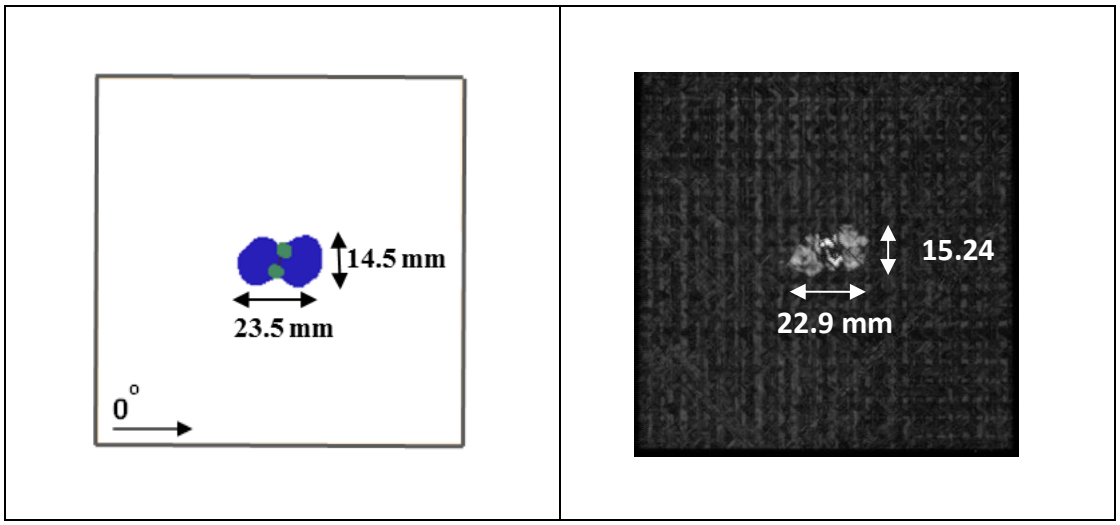

(b): Left hand side – LS-DYNA /UMAT41 simulation, Right hand side - NDE measurements.

Figure 9: Overall delamination of NCF laminate for a 5J impact load.

10J Impact Energy

The load history curves and delamination damage obtained from the ABAQUS/COSTR PFA were compared with the four experiments with 10J impact energy and are presented in Figure 10.

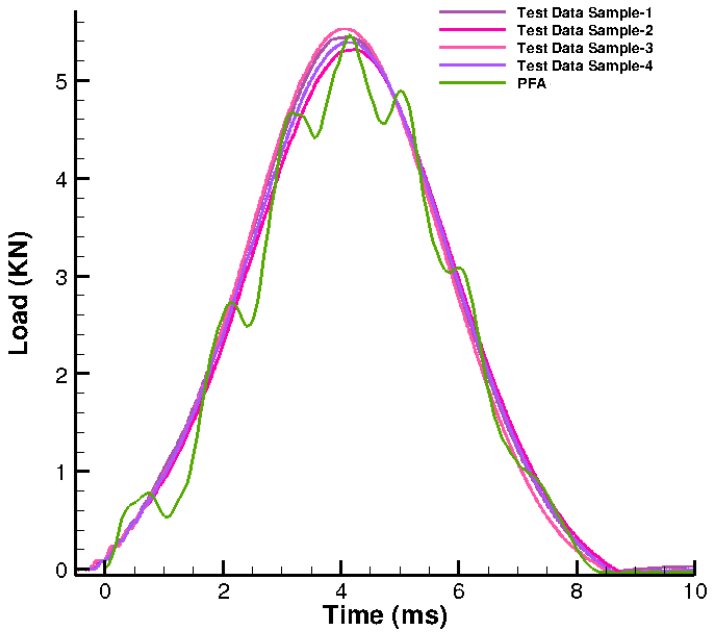

Figure 10: Load history curve for 10J impact energy case.

It can be seen from the figure that the contact duration and the impact load obtained from the analysis are in very good agreement with the test data. Similar to the 5J impact energy case, the load history curve obtained from the analysis was oscillatory, and by passing through the multi-pass filters provided in the ABAQUS post processing tool, these oscillations were smoothed out.

The delamination at certain critical ply interfaces for the 10J impact load is presented in Figure 11. The ultrasound scans for this specimen were taken looking up from the bottom, starting from the 8^{th} layer (non-impact side). The general orientation of the delamination at the interface of layers 6-7 was predicted fairly well. However the NDE data at other interfaces show poor correlation with the simulation, but this may be due to the masking effect of the damage at the interface of layers 6-7. The areas of cumulative delamination of the laminate, determined from PFA, and the experimental measurements from the NDE ultrasound are presented in Figure 12. These show a good agreement and are a better assessment of the total damage area in the laminate.

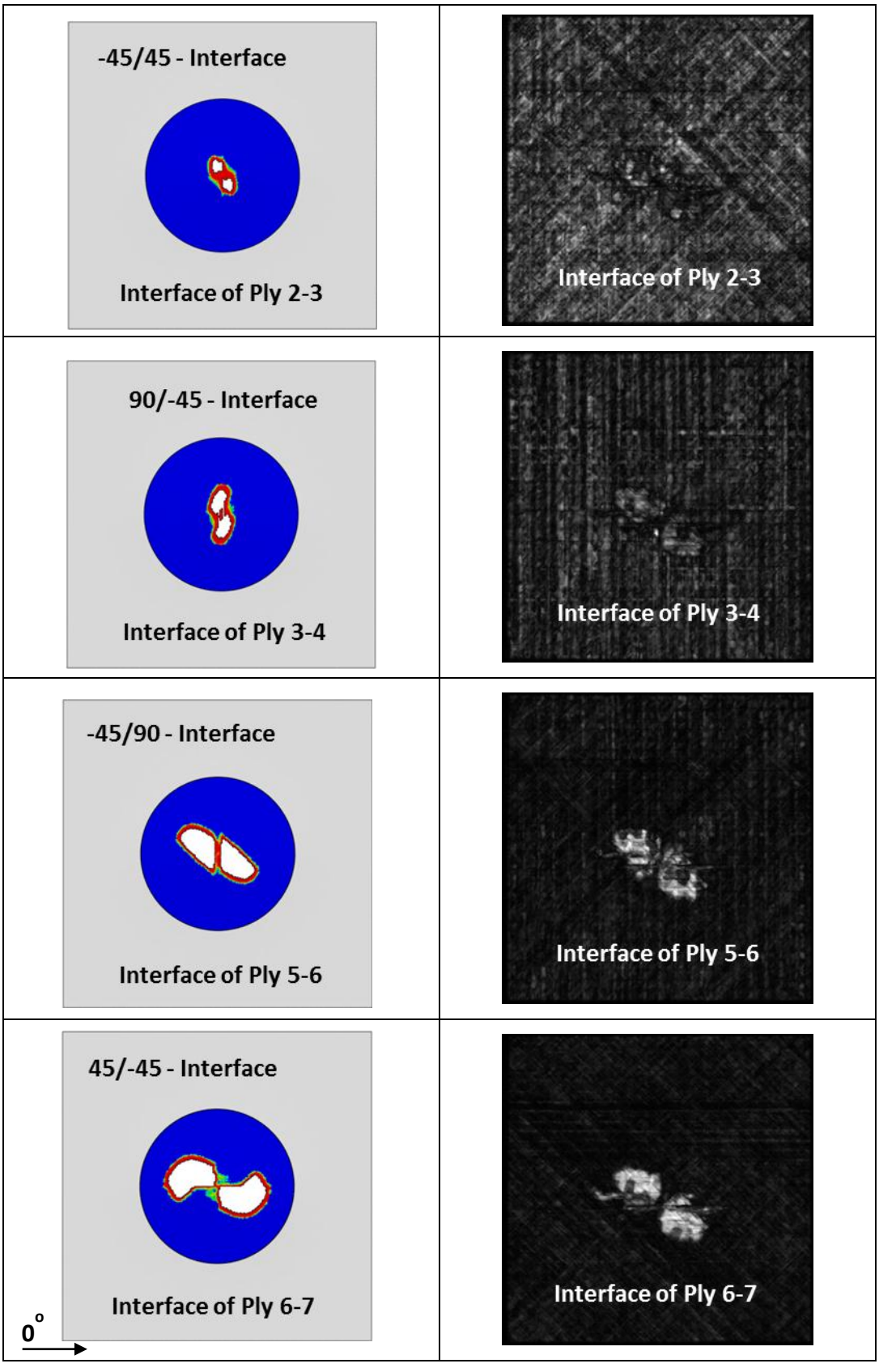

Figure 11: Delamination at certain interfaces. Left hand side - PFA, Right hand side - NDE technique.

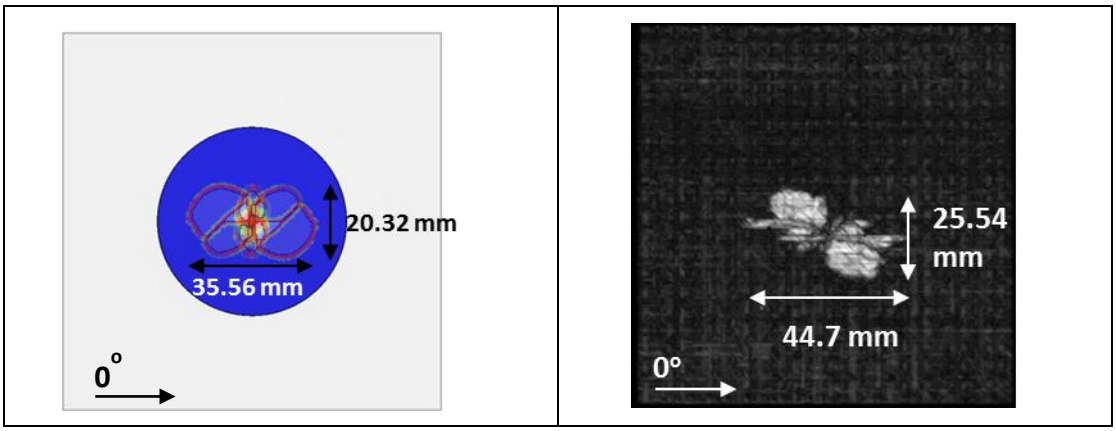

Figure 12: Overall delamination of NCF laminate for a 10J impact load. Left hand side - PFA, Right hand side - NDE technique.

For the 10J impact energy level, a significant amount of matrix damage was predicted in all of the plies as presented in Figure 13. The region with matrix damage is indicated in red and the undamaged regions are indicated in blue. The matrix damage predicted in the plies is due to the in-plane transverse tension/compression stress, or shear stresses, reaching the failure limit either individually or in combination. From Figure 13, it is seen that the matrix damage was occurring parallel to the fibers in the 0^o and 90^o plies (see the layer-8 and layer-4&5 plots). However for the 45^o plies, the damage was oriented parallel to, or and at some angle to the fibers (see the layer-6 and layer-3 plots). No fiber damage was predicted in any of the plies in the simulation and none was observed in the experiments.

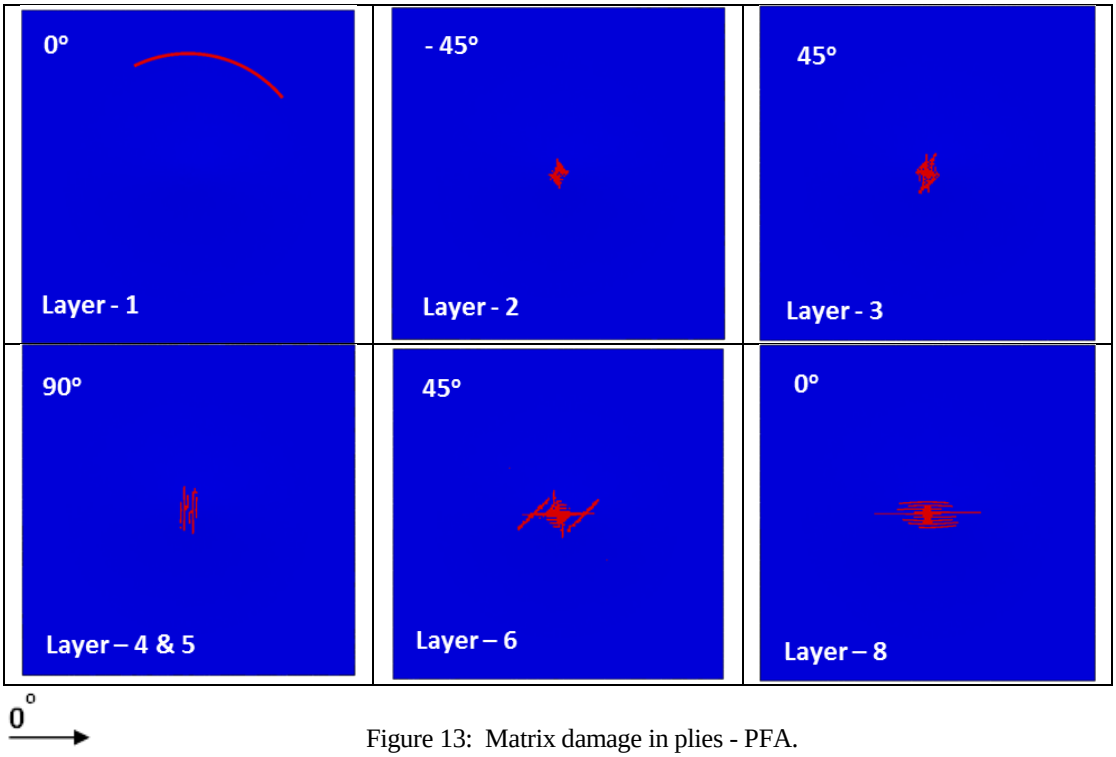

Figure 13: Matrix damage in plies - PFA.

12J Impact Energy

The load history curves obtained from PFA and four experiments for the impact test case of 12J energy level are presented in Figure 14. The magnitude of the impact load and the contact duration from the simulations are in good agreement with

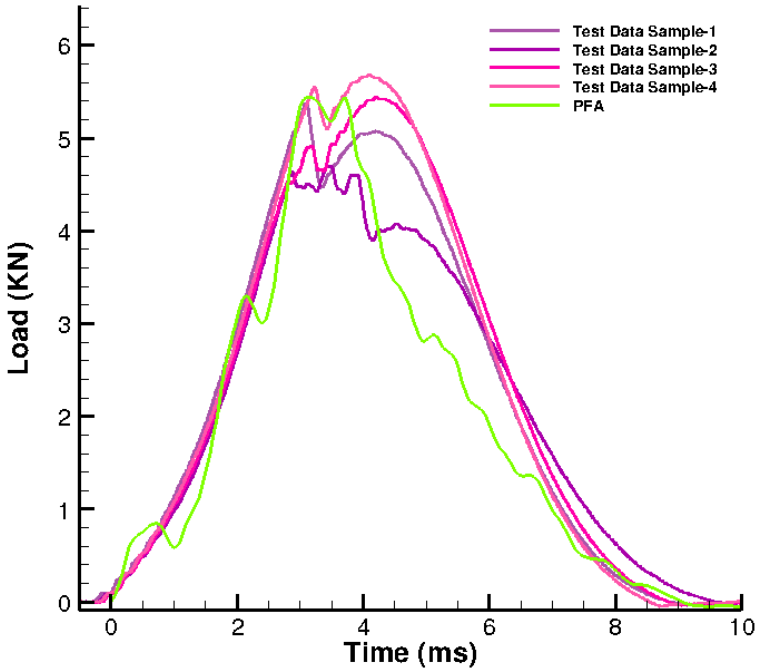

Figure 14: Load history curve for 12J impact energy case.

the test data. The NCF plate had extensive matrix damage in all of the plies and fiber failure in some plies. The test data shown in Figure 13 indicates that this damage occurs at around 3.1 milliseconds, accompanied by a load drop. The PFA simulation predicts similar behavior in the load history curve.

The delamination at certain critical ply interfaces for the 12J impact load is presented in Figure 15. As the non-destructive evaluation results for the delamination damage at each of the interfaces was not available, only simulation results are presented. The cumulative delamination damage in the NCF plate predicted from the PFA was compared with the NDE results and is presented in Figure 16. From this figure, we can see a good agreement in the overall size of the delamination between the PFA and experimental results. The length of delamination damage from the test data (69 mm) was larger than the predicted delamination from the PFA data. This is due to the fact that few fiber tows in the outer layer of the laminate from the non-impact side debonded from the rest of the laminate and the PFA was unable to capture this phenomenon as layers 7 & 8 were modeled with one element in the thickness direction thereby restricting the relative displacement between them. However, the delamination damage in the rest of the plies matches well with the PFA data. Again, as mentioned in the previous sections, the white region indicates a complete delamination of the interfaces, the red region indicates areas which are 95% of complete delamination of the interface, and the blue region denotes intact bonding of the interfaces.

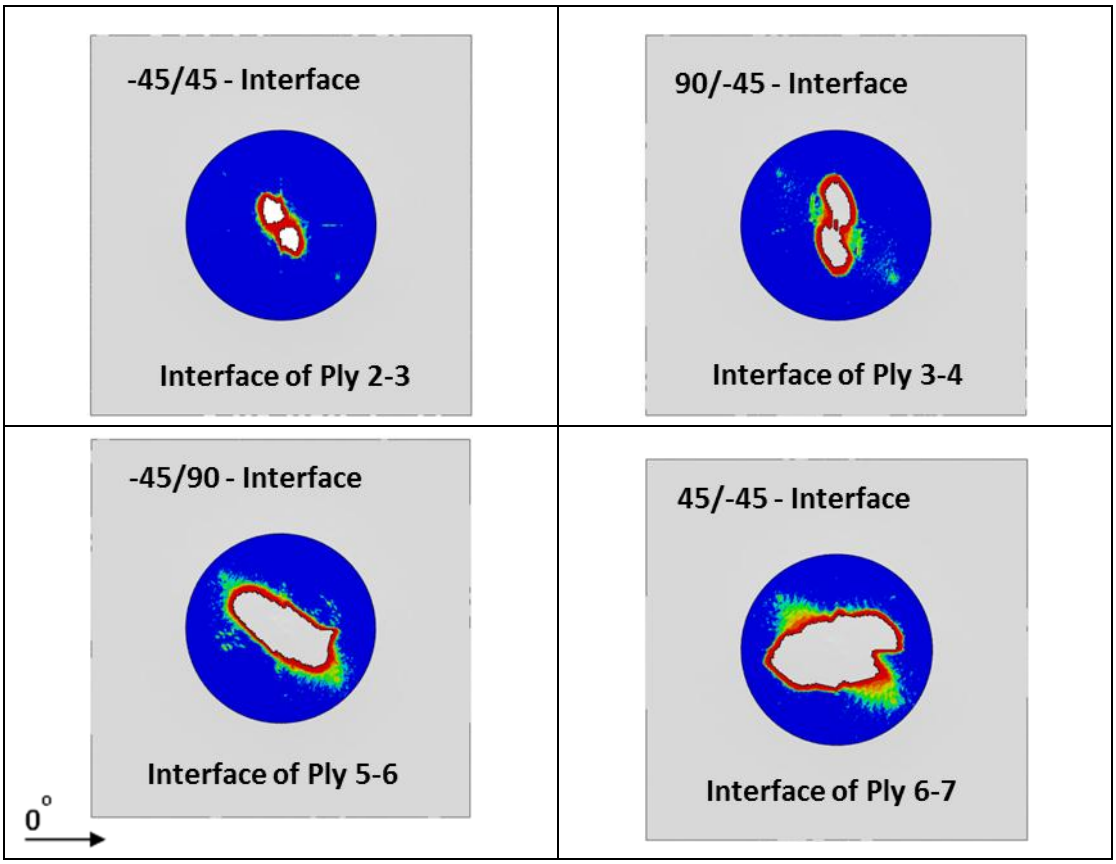

Figure 15: Delamination at certain interfaces. Left hand side - PFA, Right hand side - NDE technique.

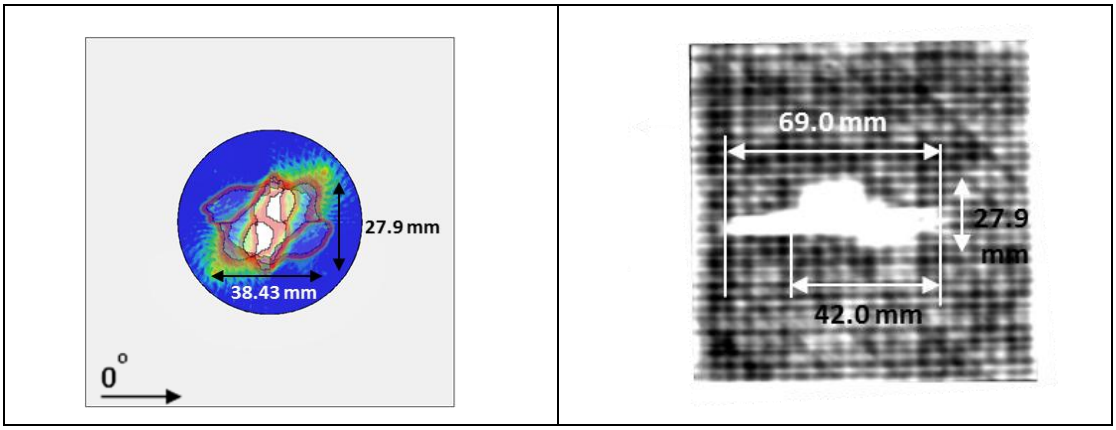

Figure 16: Overall delamination of NCF laminate for a 12J impact load. Left hand side - PFA, Right hand side - NDE technique.

For the 12J impact energy level, a significant amount of matrix damage was predicted from the PFA in all the plies, and is presented in Figure 17. The region with matrix damage is indicated in red while the undamaged regions are indicated in blue. It can be observed from Figure 17 that the matrix damage is again occurring parallel to the fibers in the 0^o and 90^o plies (see layer-8, layer-4&5). However, in the 45^o plies

(layer-2 and layer-3) , the damage is oriented in parallel to, or at some angle relative to the fibers. Note the circumferential damage in layer-1 at the circular clamping boundary.

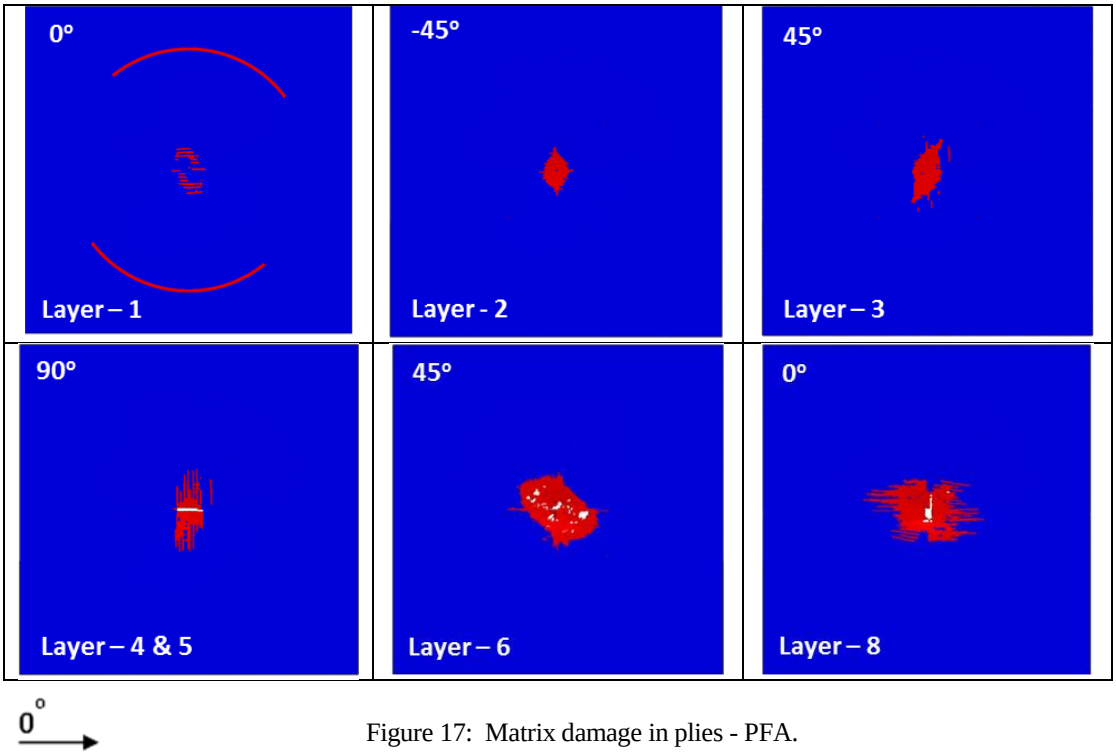

Figure 17: Matrix damage in plies - PFA.

Figure 18 presents the comparison of fiber damage in the outer 5 plies (from layer-4 to layer-8 where layer- 8 is the bottom most layer) predicted from simulation and CT scan measurements. Complete fiber failure regions are indicated in white and partial fiber failure areas are indicted in blue. Undamaged areas are indicated in red. Note from the figure that the fiber damage predicted in the simulation (white regions) matches well with the fiber failure determined from the CT scan data. The fiber damage in layers 7 & 8 are identical in shape and size in the simulation due to the fact that the relative displacements between these two layers have been restricted on account of modeling procedure adopted in this work.

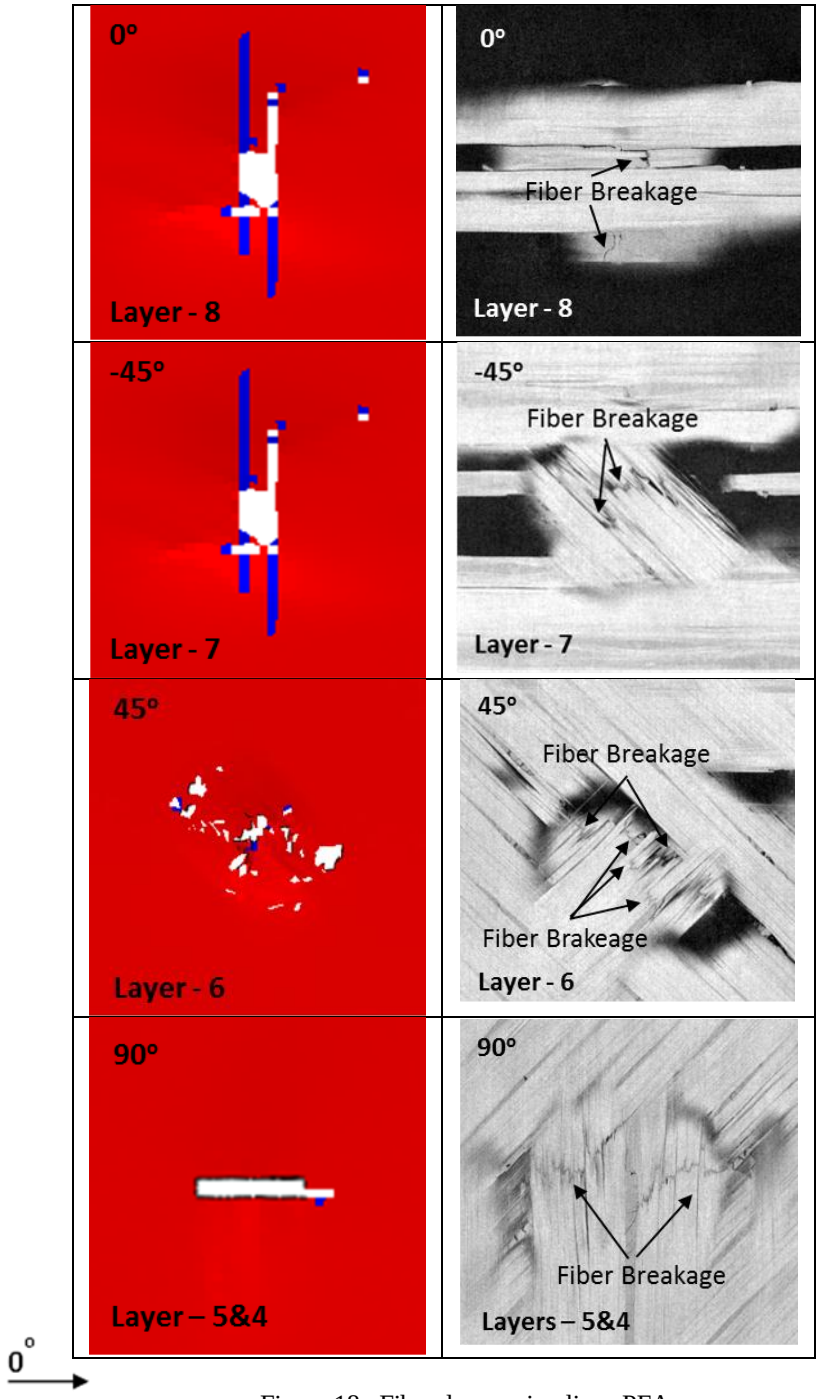

Figure 18: Fiber damage in plies - PFA.

CONCLUSION

Low velocity impact tests and progressive failure analysis of thin NCF laminated composites were successfully performed for 5J, 10J and 12J energy levels. The Complete Stress Reduction (COSTR) damage model was newly implemented in the LS-DYNA framework using a user subroutine based on the previous ABAQUS/VUMAT implementation. Both of the implementations were assessed in predicting the fiber, matrix, and delamination damages under the low velocity

transverse impact and found to be in good agreement with the damage identified through NDE technique used during testing.

ACKNOWLEDGEMENTS

X-ray CT and ultrasound scans were provided by NASA Langley's Nondestructive Evaluation Branch, who are also part of NASA-GM partnership team, and the authors gratefully acknowledge Daniel Perey and Eric Burke for their support.

REFERENCES

1. Asp, E. L., "Local Models for NCF Composite Materials Mechanical Performance Prediction", proceedings of 16th International Conference on Composite Materials, Kyoto, Japan, 2007.
2. Oakeshott, L. J., Iannucci, L., & Robinson, P., "Development of a Representative Unit Cell Model for Bi-Axial NCF Composites", Journal of Composite Materials, 2007, Vol. 41, No. 7, pp. 801-835.
3. Athreya, R. S., Ma, L., Barpanda, D., Jacob, G., & Verghese, N., "Estimation of in-plane elastic properties of stitch-bonded, non-crimp fabric composites for engineering applications", Journal of Composite Materials, 2012, Vol. 48(2), pp. 143-154.
4. Edgren, F., Mattson, D., Asp E. L., & Varna J., "Formation of damage and its effects on non-crimp fabric reinforced composites loaded in tension", Composites Science and Technology, Vol.64, 2004, pp. 675-692.
5. Joffe, R., Mattson, D., Modniks, J., & Varna, J., "Compressive failure analysis of non-crimp fabric composites with large out-of-plane misalignment of fiber bundles", Composites: Part A, Vol. 36, 2005, pp. 1030-1046.
6. Edgren, F., Asp, E. L., & Bull, H. P., "Compressive Failure of Impacted NCF Composite Sandwich Panels-Characterization of the Failure Process", Journal of Composite Materials, Vol. 38, No. 6, 2004.
7. Montemurro, P. M., Hansen, S. J., & Houde, L. J. M., "Finite Element analysis of the Impact Response of Composite Plates and Shells", Proceedings of the AIAA/ASME/ASCE/AHS/ASC 39th Structures, Structural Dynamics & Materials Conference, AIAA paper No. 93-1448-CP, pp. 1245-1253, 1993.
8. Yen, C. F., and Cassin, T., "Progressive Failure Analysis of Thin Walled Composite Tubes under Low Energy Impact," Proceedings of the AIAA/ASME/ASCE/AHS/ASC 39th Structures, Structural Dynamics & Materials Conference, AIAA paper No. 98-1742, pp. 363-371, 1998.
9. Heimbs, S., Heller, S., & Middendorf, P., "Simulation of Low Velocity Impact on Composite Plates with Compressive Preload", Material II – Composites, Proceedings of the 7th LS-DYNA Anwenderforum, Bamberg, Germany, 2008.
10. Lopes, C., Gurdal, G., Camanho, P. P., Maimi & Gonzalez, V. E., "Simulation of Low-Velocity Impact Damage on Composite Laminates", Proceedings of the AIAA/ASME/ASCE/AHS/ASC 50th Structures, Structural Dynamics & Materials Conference, AIAA paper No. 2009-2445, 2009.
11. Kim, Ho-Eun, Lee-In, & Hwang, Kyung-Tae., "Low-Velocity Impact and Residual Burst-Pressure Analysis of Cylindrical Composite Pressure Vessels", AIAA Journal, Vol. 50, No. 10, pp. 2180-2193, 2012.
12. Satyanarayana, A., Bogert, P., Karayev, Z. K., Nordman, S. P., & Hamid, R., "Influence of Finite Element Size in Residual Strength Prediction of Composite Structures", Proceedings of the 53rd AIAA/ASME/ASCE/AHS/ASC Structures, Structural Dynamics & Materials Conference, AIAA paper No. 2012-1619, 2012.
13. ABAQUS User's Manual, Vol. 1-3, Version 6.4, Hibbitt, Karlsson, and Sorensen, Pawtucket, RI.
14. Christy, C., " Numerical Modeling of a Propagating Crack", Master Thesis, Naval Postgraduate School, Monterey, CA 93943, thesis No. 93-27957, June 1993.
15. LS-DYNA User's Manual, Volume II, Livermore Software Technology Corporation, 7374 Las Poistas Road, Livermore, CA-94550.
16. Turon, A.; Dávila, C. G.; Camanho, P. P.; and Costa, J.: "An Engineering Solution for Mesh Size Effects in the Simulation of Delamination Using Cohesive Zone Models." Engineering Fracture Mechanics, Vol. 74, No. 10, 2007, pp. 1665-1682, doi: 10.1016/j.engfracmech.2006.08.025.